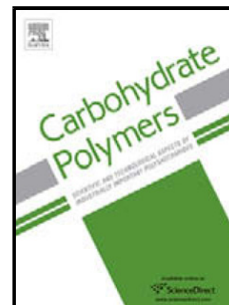


Journal Pre-proof

Metformin and Berberine suppress glycogenolysis by inhibiting glycogen phosphorylase and stabilizing the molecular structure of glycogen in *db/db* mice



Xiaocui Liu (Investigation) (Writing - original draft), Kaiping Wang (Investigation) (Project administration), Jing Zhou (Validation), Mitchell A. Sullivan (Writing - review and editing), Yage Liu (Investigation), Robert G. Gilbert (Supervision), Bin Deng (Conceptualization) (Funding acquisition) (Supervision)

PII: S0144-8617(20)30609-3

DOI: <https://doi.org/10.1016/j.carbpol.2020.116435>

Reference: CARP 116435

To appear in: *Carbohydrate Polymers*

Received Date: 23 December 2019

Revised Date: 18 April 2020

Accepted Date: 8 May 2020

Please cite this article as: Liu X, Wang K, Zhou J, Sullivan MA, Liu Y, Gilbert RG, Deng B, Metformin and Berberine suppress glycogenolysis by inhibiting glycogen phosphorylase and stabilizing the molecular structure of glycogen in *db/db* mice, *Carbohydrate Polymers* (2020), doi: <https://doi.org/10.1016/j.carbpol.2020.116435>

This is a PDF file of an article that has undergone enhancements after acceptance, such as the addition of a cover page and metadata, and formatting for readability, but it is not yet the definitive version of record. This version will undergo additional copyediting, typesetting and review before it is published in its final form, but we are providing this version to give early visibility of the article. Please note that, during the production process, errors may be discovered which could affect the content, and all legal disclaimers that apply to the journal pertain.

© 2020 Published by Elsevier.

Metformin and Berberine suppress glycogenolysis by inhibiting glycogen phosphorylase and stabilizing the molecular structure of glycogen in *db/db* mice

Xiaocui Liu^{a#}, Kaiping Wang^{a#}, Jing Zhou^b, Mitchell A. Sullivan^c, Yage Liu^a, Robert G. Gilbert^{d,e}, Bin Deng^{b*}

^a Hubei Key Laboratory of Natural Medicinal Chemistry and Resource Evaluation, School of Pharmacy, Tongji Medical College, Huazhong University of Science and Technology, 430030, Wuhan, China

^b Department of Pharmacy, Union Hospital, Tongji Medical College, Huazhong University of Science and Technology, Wuhan, Hubei 430030, China

^c Glycation and Diabetes Group, Mater Research Institute-The University of Queensland, Translational Research Institute, Brisbane, Queensland 4072, Australia

^d Joint International Research Laboratory of Agriculture and Agri-Product safety, College of Agriculture, Yangzhou University, 225009, Yangzhou, Jiangsu Province, China

^e Centre for Nutrition and Food Sciences, Queensland Alliance for Agriculture and Food Innovation, The University of Queensland, Brisbane, Queensland, 4072, Australia

both are equal first author

* Corresponding author at: Department of Pharmacy, Union Hospital, Tongji Medical College, Huazhong University of Science and Technology, Wuhan, Hubei 430030, China

E-mail addresses: dengbin@hust.edu.cn

Highlights

- Structural analysis of glycogen was obtained with SEC, FACE and TEM
- The structural changes of diabetic glycogen are found under two drugs treatments
- The changed glycogen structure could have influence on the rate of glycogenolysis
- Metformin and berberine efficiently decrease the affinity of glycogen with GP
- The increased GP level in diabetic mice declined under two drugs treatments

Abstract

Glycogen is a branched glucose polymer involved in sustaining blood glucose homeostasis. Liver glycogen comprises α particles (up to 300 nm in diameter) made of joined β particles (~20 nm in diameter). Glycogen α particles in a mouse model for diabetes are molecularly fragile, breaking down into smaller β particles more readily than in healthy mice. Glycogen phosphorylase (GP), a rate-limiting enzyme in glycogen degradation, is overexpressed in diabetic mice. This study shows that Metformin and Berberine, two common drugs used to treat diabetes, are able to revert the liver glycogen of diabetic mice to the stable structure seen in non-diabetic mice. It is also shown that these drugs reduce the GP level via the cAMP/PKA signaling pathway in diabetic livers and decrease the affinity of GP with the glycogen of *db/db* mice. These effects of these drugs may slow down the degradation of liver glycogen and improve glucose homeostasis.

Abbreviations

GP: glycogen phosphorylase; BBR: berberine; MET: metformin; T2DM: type 2 diabetes mellitus; DMSO: dimethyl sulfoxide; FBG: fasting blood glucose; GDBE: glycogen debranching enzyme; TBST: Tris Buffered Saline Tween; G-6-Pase: glucose-6-phosphatase;

PEPCK: phosphoenolpyruvate carboxykinase; GS: glycogen synthase; GBE: glycogen branching enzyme; GPCR: G protein-coupled receptor; cAMP: cyclic adenosine monophosphate; PKA: protein kinase A; PK: glycogen phosphorylase kinase; HNF-4 α : hepatocyte nuclear factor-4 α ; AMPK: adenosine 5'-monophosphate (AMP)-activated protein kinase; GAPDH: glyceraldehyde 3-phosphate dehydrogenase; SEC: size-exclusion chromatography; FACE: fluorescence assisted carbohydrate electrophoresis; CLD: chain length distribution; ACL: average chain length; K_m : Michaelis constant; V_{max} : Michaelis maximum velocity.

Keywords: Glycogen, Diabetes, Metformin, Berberine, Glycogen phosphorylase, Molecular structure

1. Introduction

Glycogen, a complex branched glucose polymer, with small amounts of functionally important protein (Deng et al., 2016), is an energy reservoir used by most organisms, allowing large quantities of glucose to be stored and released when needed. In mammals, glycogen is formed in various organs, with its role being tissue-specific. For example, skeletal glycogen and cardiac glycogen act as a supply of energy for muscle contraction, brain glycogen sustains neuronal activity and promotes cognitive processes (Duran, Gruart, Varea, Lopez-Soldado, Delgado-Garcia & Guinovart, 2019), while liver glycogen acts as a blood-glucose buffer to maintain glucose homeostasis (Ellingwood & Cheng, 2018). When blood glucose levels increase after a meal, a significant portion of this glucose will be transferred to the liver and

stored as glycogen. This liver glycogen will then be degraded into glucose to supply the blood during periods of fasting (Petersen, Vatner & Shulman, 2017).

Diabetes, currently affecting over 420 million people worldwide, characteristically involves a breakdown in the ability to regulate blood glucose levels (International Diabetes Federation, 2019). It has been demonstrated that hepatic glycogen metabolism is dysregulated in both type 1 and type 2 diabetes mellitus (Petersen, Vatner & Shulman, 2017), contributing to diabetes-associated hyperglycemia.

Hepatic glucose production accounts for more than 90% of endogenous glucose production, and mostly comes from glycogenolysis and gluconeogenesis (Petersen, Vatner & Shulman, 2017). Glycogenolysis releases glucose into the bloodstream for uptake by other cells and is regulated hormonally in response to blood glucose levels by glucagon and insulin (Liu et al., 2019). Glycogen phosphorylase (GP), a rate-limiting enzyme in glycogenolysis, catalyzes the degradative phosphorylation of terminal glycosyl units in glycogen to glucose-1-phosphate (Stathi, Mamais, Chrysina & Gimisis, 2019). This enzyme is activated when the inactive form, GP_b, is phosphorylated at serine 14, becoming the active GP_a (Agius, 2015). It has been demonstrated that GP_a levels are abnormally elevated under diabetic conditions (Oyenihi, Langa, Mukaratirwa & Masola, 2019). As a result, glycogenolysis and hepatic glucose production in diabetes are significantly elevated relative to that without diabetes (Boden, 2004). Thus, suppressing glycogenolysis to reduce hepatic glucose output has been considered an effective approach to ameliorate hyperglycemia. Moreover, the design of

specific inhibitors of GP, in order to prevent glycogenolysis under high blood glucose conditions, is seen as a promising therapeutic target for diabetes (Barr et al., 2019).

In addition to changes in the level of GP in diabetes, the molecular structure of liver glycogen has also been shown to be altered with the disease. Glycogen structure is often described at three different levels: 1) single chains are composed of glucose units that are connected by (1→4)- α glycosidic bonds; 2) these single chains are joined together through (1→6)- α glycosidic bonds (branch points) to comprise branched β particles (~20 nm in diameter); 3) these β particles can join together to form α particles (up to 300 nm in diameter) (Rybicka, 1996). We have found that the bonding between β particles in α particles in *db/db* mice, a commonly-used animal model for diabetes, is more fragile than that in non-diabetic mice, when exposed to a hydrogen-bond disruptor (dimethyl sulfoxide) (Deng et al., 2015); moreover, liver glycogen in diabetic mice has longer polymeric glucose chains and a higher molecular density compared with non-diabetic mice (Hu et al., 2018). The enzymatic degradation rate of β particles was demonstrated to be significantly faster *in vitro*, most likely due to their higher surface area to volume ratio (Jiang et al., 2016). Therefore, the fragile nature of α particles in diabetic livers could result in accelerated glycogen degradation, elevated hepatic glucose production and uncontrolled blood glucose levels. Repairing the impaired (fragile) structure of liver glycogen may therefore be an approach to suppress glycogenolysis and decrease hepatic glucose output.

Metformin (MET) is one of the first-line oral antidiabetic drugs for the clinical treatment of type 2 diabetes mellitus (T2DM). Berberine (BBR), an active quaternary ammonium salt

extracted from *Coptis chinensis Franch*, exhibits hypoglycemic effects and has been widely recognized as an active ingredient that could be possibly developed into a new anti-diabetes drug (Chang, Chen & Hatch, 2015). Although the efficacy of MET and BBR has been widely demonstrated, the hypoglycemic mechanisms have not been elucidated comprehensively. The anti-diabetic mechanisms of both drugs appear to be quite similar: both can promote insulin secretion, improve the expression of insulin receptors and insulin sensitivity, inhibit gluconeogenesis, activate glycolysis and increase hepatic glucose uptake (Chang, Chen & Hatch, 2015; Zhou, Xu, Du, Zhao & Wang, 2018). However, studies that focus on the effect of MET and BBR on glycogenolysis are rare. It has, however, been reported that MET could decrease the activity of GP in a type 2 diabetes animal model (Jayanthi & Subramanian, 2014). In addition, our previous study demonstrated that BBR could increase the amount of stable α particles in the liver glycogen of diabetic mice (Li et al., 2019). Based on the apparent similarities of the anti-diabetic mechanism between MET and BBR, we hypothesize that both MET and BBR can suppress glycogenolysis by regulating GP and modifying liver glycogen molecular structure simultaneously.

In the present study, we analysed the effects of MET and BBR treatment on α particle stability and other aspects of glycogen molecular structure in *db/db* mice and investigated the effects of these drugs on GP and its upstream pathways. This study aims to reveal more details on the mechanism whereby MET and BBR inhibit glycogenolysis and reduce hepatic glucose production. The findings of this study will provide some new knowledge on the hypoglycemic

mechanisms of MET and BBR and will act as a reference for mechanistic studies of other anti-diabetic drugs.

2. Materials and methods

2.1. Materials

Metformin hydrochloride tablets (H20023370, Sino-US Shanghai Squibb Pharmaceutical Co., Ltd, China) and berberine hydrochloride tablets (H21022453, Northeast Pharmaceutical Group Co., Ltd, China) were obtained from Union Hospital, Tongji Medical College, Huazhong University of Science and Technology, Wuhan, China.

2.2. Animal experiments

All animal experiments were approved by the institutional Animal Care and Use Committee of Tongji Medical College, Huazhong University of Science and Technology (IORG no. 0003571). The animal care and experimental procedures were carried out in accordance with the Guidelines of the Institutional Animal Care and Use Committee of Tongji Medical College and the National Institutes of Health Guide for the Care and Use of Laboratory Animals. Male mice on a C57BL/6JNju background (8 weeks) were purchased from the Hubei Provincial Center for Food and Drug Safety. Male mice on C57BL/BKS-Lepr^{em2Cd479}/Nju (C57BL/6JNju-*db/db*, genotyping is (Lepr^{db}) mut/mut) background (8 weeks) were purchased from the Model Animal Research Center of Nanjing University. Mice were bred in a SPF room with standard cages (4 mice/cage) under the following conditions: 22 ± 1 °C, a 12-h dark-light cycle. All

animals had ad libitum access to water and standard chow (6% kcal from fat, 14.3 MJ kg⁻¹, Hubei Provincial Center for Disease Control and Prevention).

After one week acclimatization, 10 healthy wild-type mice and 30 *db/db* mice were randomly divided into 4 groups: Group A (NC): healthy mice treated with distilled water; Group B (DC): diabetic mice treated with distilled water; Group C (MET): diabetic mice treated with metformin (300 mg/kg/d); Group D (BBR): diabetic mice treated with Berberine (300 mg/kg/d) (Chang, Chen & Hatch, 2015; Zhou, Xu, Du, Zhao & Wang, 2018). Drug treatment lasted for 8 weeks.

At the end of the experiment, the mice were fasted overnight and anaesthetized with sodium pentobarbitone (150 mg/kg in traperitoneal). Blood samples of all mice were collected and immediately separated by centrifugation (1200 × *g*, 4 °C, 15 min) to obtain the serum. The liver tissues were collected in microtubes and snap frozen in liquid nitrogen. Samples were stored at -80 °C until assayed.

2.3. *Body weight, water intake, food intake and FBG*

Body weight, water intake and food intake were measured at the beginning and end of the experiment. All mice were fasted for 8 h, and then fasting blood glucose (FBG) levels were determined from the tail veins of mice using a blood glucose meter (Contour TS, BAYER, Germany) every week.

2.4. Biochemical analysis

The glucagon level and insulin content in the serum were measured by a glucagon ELISA kit (H183, Nanjing Jian Cheng Bioengineering Institute, China) and insulin ELISA kit (Shanghai Jianglai Industrial Limited By Share Ltd, China). The activities of GP, glycogen synthase (GS), glycogen debranching enzyme (GDBE), glucose-6-phosphatase (G-6-Pase) and phosphoenolpyruvate carboxykinase (PEPCK) in liver tissue were examined by GP assay kit (BC3345, Beijing Solarbio Science & Technology Co., Ltd, China), GS assay kit (Shanghai Jianglai Industrial Limited By Share Ltd, China), GDBE assay kit (JL48081, Shanghai Jianglai Industrial Limited By Share Ltd, China), G-6-Pase assay kit (JL20500, Shanghai Jianglai Industrial Limited By Share Ltd, China) and PEPCK assay kit (JL20462, Shanghai Jianglai Industrial Limited By Share Ltd, China), respectively. The level of cAMP (cyclic adenosine monophosphate) in liver tissue was determined by a cAMP ELISA kit (JL20462, Shanghai Jianglai Industrial Limited By Share Ltd, China). All experimental procedures were carried out following the manufacturer's instructions.

2.5. Western Blots

Western blots were performed as previously described (Liu, Wang, Li, Wu, Liu & Wu, 2004; Wang et al., 2018). Three liver samples of each group were examined as follows. Total protein was extracted from liver tissue in RIPA lysis buffer (25 mM Tris-HCl, 25 mM NaCl, 0.5 mM EDTA, 1% Triton X-100 and 0.1% SDS) containing 1% PMSF protease inhibitors (P1005, Beyotime Biotechnology, China) and phosphatase inhibitors (P1081, Beyotime Biotechnology, China), and the protein concentration was measured by bicinchoninic acid

(BCA) protein assay kit (P0012S, Beyotime Biotechnology, China). Equal amounts of protein were separated by 10-15% SDS-PAGE and then transferred to PVDF (poly(vinylidene difluoride)) transfer membranes (IPVH00010, Millipore, Germany). After blocking with Tris Buffered Saline Tween (TBST) for 3 h, the membranes were incubated with the primary antibodies overnight at 4 °C. Then, the membranes were washed 3 times with TBST and incubated with the secondary antibodies for 1 h at room temperature. After washing with TBST for a further three times, the protein bands were visualized by enhanced chemiluminescence (32134, Thermo, USA) solution and imaged with Automated Imaging System (Gene Gnome5, Synoptics Ltd, UK). GAPDH (glyceraldehyde 3-phosphate dehydrogenase) was assumed to be similarly abundant in all samples and was used as a loading control. The primary antibodies were anti-GPCR (ab171065, Abcam, US), anti-PKA (#4782, Cell Signaling Technology, USA), anti-PK (ab176338, Abcam, US), anti-p-PK (ab194112, Abcam, US) anti-GPa (ab223788, Abcam, UK), anti-HNF4- α (ab181604, Abcam, UK), anti-p-AMPK (ab133448, Abcam, UK), anti-AMPK (ab80039, Abcam, UK), anti-GS (ab40810, Abcam, UK), anti-p-GS (ab81230, Abcam, UK), anti-GBE (glycogen branching enzyme, ab180596, Abcam, UK), anti-glycogenin (sc-271109, Santa Cruz Biotechnology, USA), anti-G-6-Pase (ab83690, Abcam, UK) and anti-PEPCK (ab187145, Abcam, UK).

2.6. Histological assessment

Periodic acid-Schiff (PAS) staining was used to observe the accumulation of glycogen in liver tissue. Three liver samples of each group were assayed as follows. A part of liver tissue was fixed in 10% formalin for 48 and then embedded in paraffin. After the paraffin was frozen,

the tissue section was cut into 4~5 μm slices and stained with periodic acid-Schiff, then observed with a light microscope (Olympus, Tokyo, Japan).

2.7. Extraction and purification of liver glycogen

The glycogen from mouse liver tissue was extracted using a density gradient centrifugation method, which has been verified to be a warm extraction method with minimal destruction of glycogen structure (Sullivan et al., 2015). Approximately 1 g of liver tissue was homogenized in 25 mL of glycogen extraction buffer (pH 8.0, 150 mM sodium chloride, 50 mM Tris, 50 mM sodium fluoride, 5 mM sodium pyrophosphate and 2 mM ethylenediaminetetraacetic acid) in an ice bath. 500 μL homogenate was removed and stored at $-80\text{ }^{\circ}\text{C}$ for subsequent use for glycogen content assessment. After centrifuging at $6000 \times g$, $4\text{ }^{\circ}\text{C}$ for 10 min, the supernatants were ultra-centrifuged at $367000 \times g$ at $4\text{ }^{\circ}\text{C}$ for 1.5 h. The pellets were resuspended in 5 mL of glycogen extraction buffer and layered above a sucrose gradient solution (10 mL of 37.5% on top of 10 mL of 75%). Then this sucrose gradient system was ultra-centrifuged at $367\ 000 \times g$, $4\text{ }^{\circ}\text{C}$ for 2 h, with the resulting pellets dissolved in 300 μL of purified water and reprecipitated in 1.5 mL of absolute ethanol. After centrifuging at $4000 \times g$, $4\text{ }^{\circ}\text{C}$ for 10 min, the precipitates were dissolved in 400 μL purified water and then lyophilized (freeze-dryer; BTP-9EL, VirTis, USA).

2.8. Liver glycogen content assays

Glycogen content in liver tissue was assessed by a glucose oxidase/oxidase (GOPOD, Megazyme, Ireland) kit as previously described (Liu et al., 2019). Briefly, 20 μL of homogenate

from the glycogen extraction process was added into a 2 mL Eppendorf tube, and 5 μL of amyloglucosidase, 100 μL of sodium acetate buffer (pH 6.0) and 475 μL of purified water were added. Then the mixture was incubated with a thermomixer at 50 $^{\circ}\text{C}$ for 30 min. A control group was prepared in the same way but with an equal volume of purified water instead of amyloglucosidase. Then a 300 μL aliquot of the mixture was transferred into 1 mL of GOPOD reagent and incubated with a thermomixer at 50 $^{\circ}\text{C}$ for 30 min. After incubation, the absorbance of the mixture at UV 510 nm was determined with a UV-vis spectrophotometer (UV-1700, Shimadzu, Japan). The glycogen content was calculated with a calibration curve, which was constructed using a series of D-glucose solutions with different concentrations (0~1 mg/mL) to react with the GOPOD reagent.

2.9. Size-Exclusion Chromatography (SEC)

SEC was used to analyze the molecular size and density distributions of liver glycogen, as previously described (Deng et al., 2015). All glycogen samples were analyzed before and after DMSO treatment. Approximately 0.5 mg of glycogen samples were dissolved in the mobile phase (50 mM sodium nitrate, 0.02% sodium azide) for 4 h at 80 $^{\circ}\text{C}$ at 1 mg/mL.

The DMSO treated samples were prepared as follows. Approximately 0.5 mg of glycogen samples were dissolved in DMSO at 1 mg/mL for 3 h at 25 $^{\circ}\text{C}$, and then absolute ethanol (at least 4 \times volume of DMSO) was added to precipitate glycogen. After centrifuging at 4000 $\times g$ for 10 min, the sediment was washed three times with absolute ethanol, dissolved with 500 μL of purified water and then lyophilized.

All samples were injected into an Agilent 1260 Infinity SEC system equipped with SUPREMA pre-column, SUPREMA 10-1000 column, SUPREMA 10-10000 column, multiple-angle laser light scattering (MALLS) detector (DAWN HELEOS-II, Wyatt, Santa Barbara, CA, USA) and refractive index detector (Optilab UT-rEX, Wyatt, Santa Barbara, CA, USA). The column temperature was set to 80 °C and the flow rate was 0.3 mL/min. To obtain a universal calibration curve, pullulan standards (Polymer Standards Services) with molar masses ranging from 342 to 2.35×10^6 Da and known hydrodynamic radii were used, which allows the conversion of elution volume to the SEC separation parameter, the hydrodynamic radius R_h . Data from DRI and MALLS detectors enable the determination of SEC weight distributions (total weight of molecules) and weight-average molecular weight (\bar{M}_w) distributions, respectively, as a function of R_h . The molecular density of glycogen was calculated using the formula $\rho(R_h) = 3 \bar{M}_w(R_h) / 4 \pi R_h^3$.

2.10. Transmission Electron Microscopy (TEM)

TEM images of glycogen were obtained by a method similar to that described elsewhere (Hu et al., 2018). Glycogen was dissolved in Tris buffer (5 mM, pH 7.0) at 0.1 mg/mL. An aliquot of 10 μ L of glycogen solution was loaded onto a carbon-coated copper grid (400 mesh) and negatively stained with 2% phosphotungstic acid for 60 s. The preparations were examined using a Hitachi H-7000 transmission electron microscope operating at 75 kV.

2.11. Fluorescence Assisted Carbohydrate Electrophoresis (FACE)

FACE was used to analyze the chain-length distribution (CLD) of liver glycogen as described previously (Hu et al., 2017). Isoamylase (E-ISAMY, Megazyme, Ireland) was used to break the (1→6)- α glycosidic bonds of glycogen, and 8-aminopyrene-1,3,6-trisulfonic acid trisodium salt (APTS; 09341, Sigma, Germany) was used to label the debranched glycogen chains. Approximately 0.5 mg of liver glycogen was dissolved in 900 μ L of warm purified water, and heated in boiling water for 10 min. After the mixture cooled to room temperature, 100 μ L of acetic acid-acetate buffer (0.1 M, pH 3.5) and 2.5 μ L of isoamylase (1000 U/mL, E-ISAMY, Megazyme, Ireland) were added. The samples were then incubated at 37 °C for 3 h and cooled to room temperature, followed by the addition of 100 μ L sodium hydroxide (0.1 M) to increase the pH to 7.0. The mixture was heated on a thermomixer at 80 °C and 350 rpm for 1 h and then lyophilized. The powder so obtained was centrifuged at 4000 g for 2 min and 1.5 μ L of APTS (0.2 M) in acetic acid (15%, v/v) and 1.5 μ L sodium cyanoborohydride (1 M) was added. After the mixture was incubated at 60 °C for 1.5 h and cooled to room temperature, 80 μ L of purified water was added to dissolve the labelled glycogen chains.

The labelled samples were detected using a PA-800 Plus FACE system (Beckman-Coulter, Brea, CA, USA) equipped with a solid-state laser-induced fluorescence detector and argon-ion laser source. Carbohydrate separation buffer was used in an N-CHO-coated capillary at 25 °C and 25 kV.

2.12. The affinity of glycogen to GP

To assay the affinity of glycogen with GP, the β -NADPH content was detected at 340 nm. This assay determines the degradation of glycogen, as detailed previously (Klinov & Kurganov, 2001). All of the kinetic reactions were performed in a 50 mM potassium phosphate buffer (pH 6.8, 1.5 mM magnesium chloride, 0.5 mM EDTA, 0.1 mM β -NADP and 0.0004% α -D-glucose-1,6-diphosphate). 20 μ L of glucose-6-phosphate dehydrogenase (G-6-PDH, 10 unit/mL), 20 μ L of phosphoglucomutase (PGLUM, 10 unit/mL), 6 μ L adenosine 5'-AMP (100 mM) and glycogen at various concentrations were incubated with 30 μ L GPb (20 unit/mL) at 37 °C for 90 min. The reaction rate was converted from the degradation of glycogen (as measured by the appearance of β -NADPH). The Lineweaver-Burk profile with a double-reciprocal plot was used to analyze the K_m of glycogen to GP (Bao et al., 2018), as shown in the Supporting Information, and the negative intercept of X-axis of each line is the K_m value of the corresponding group.

2.13. Statistical analysis

SPSS 19.0 was used for all statistical analysis. All of the results are expressed as the mean \pm S.D. Data were analyzed by one-way ANOVA and Dunnett's T test. P values of less than 0.05 were considered to statistically significant.

3. Results and discussion

3.1. Effects of MET and BBR on body weight, food and water intake, FBG, glucagon and insulin

in db/db mice

The body weight changes of each group during the experiment are displayed in **Fig. 1A**. The body weights of *db/db* mice were substantially higher than that of the NC group, which is the expected phenotype of these mice (Wang & Brubaker, 2002). During the experiment, the diabetic mice tended to gain more weight than the non-diabetic mice, due to the mutation of their leptin receptor (Wua, Wang, Li & Men, 2013). However, MET could slightly limit the *db/db* mice from gaining more weight, while BBR could even lower the body weight of *db/db* mice. These data indicate MET and BBR could to some extent inhibit the weight gain of *db/db* mice.

The food intake and water intake of all groups are shown in **Fig. 1B, C**. The mice in each group had ad libitum access to water and standard chow during the entire drug-treatment experiment. As shown in **Fig. 1B, C**, the food and water intake of the BBR group decreased by 48.9% and 54.3%, respectively, and those of the MET group decreased by 55.0% and 66.2%, respectively, compared to their intake at the beginning of the study. This indicates that MET and BBR reduce food intake and water intake in *db/db* mice, which might be a reason for the reduction in their body weight gain.

Fig. 1D, E show the FBG levels of each group across various time points of the experiment. As expected (Chang, Chen & Hatch, 2015; Zhou, Xu, Du, Zhao & Wang, 2018), the FBG at the end of experiment of the MET and BBR groups were significantly decreased, by 24.4% and 30.3%, respectively, compared with their initial FBG. The data here further confirmed the significant hypoglycemic effect of MET and BBR.

Glucagon, a hormone secreted by islet α cells, plays a critical role in glucose homeostasis and in multiple ways has the opposite effect to insulin (Girard, 2017). It has been demonstrated that glucagon levels are abnormally elevated under diabetic conditions, and that excessive glucagon secretion partly contributes to diabetic hyperglycemia (Hansen & Johansen, 1970). As shown in **Fig. 1F**, the serum glucagon levels of diabetic mice were significantly higher than that of non-diabetic mice. After treatment with MET and BBR, the glucagon levels in *db/db* mice were decreased by 23.2% and 22.7%, respectively, compared with the DC group (**Fig. 1F**). This result suggests that both MET and BBR could inhibit glucagon secretion in diabetic mice, potentially ameliorating hyperglycemia via the regulation of glucagon.

Insulin is an important hormone secreted by islet β cells that results in a lowering of blood glucose levels. (Thevis, Thomas & Schänzer, 2010). In diabetic mice, insulin receptors have been reported to be relatively insensitive to insulin, which leads to a compensatory increase in insulin levels to regulate blood glucose levels (Balbaa, El-Zeftawy, Ghareeb, Taha & Mandour, 2016). The Homeostatic Model Assessment of Insulin Resistance (HOMA-IR) is a method used for measuring insulin resistance (Liu et al., 2019). As shown in **Fig. 1G, H**, the serum insulin level and HOMA-IR in diabetic mice were significantly higher than in non-diabetic mice, demonstrating insulin resistance in the *db/db* mice. After the treatment with MET and BBR, both the insulin levels and HOMA-IR in *db/db* mice were clearly decreased. These results indicate that MET and BBR might alleviate insulin resistance seen in *db/db* mice.

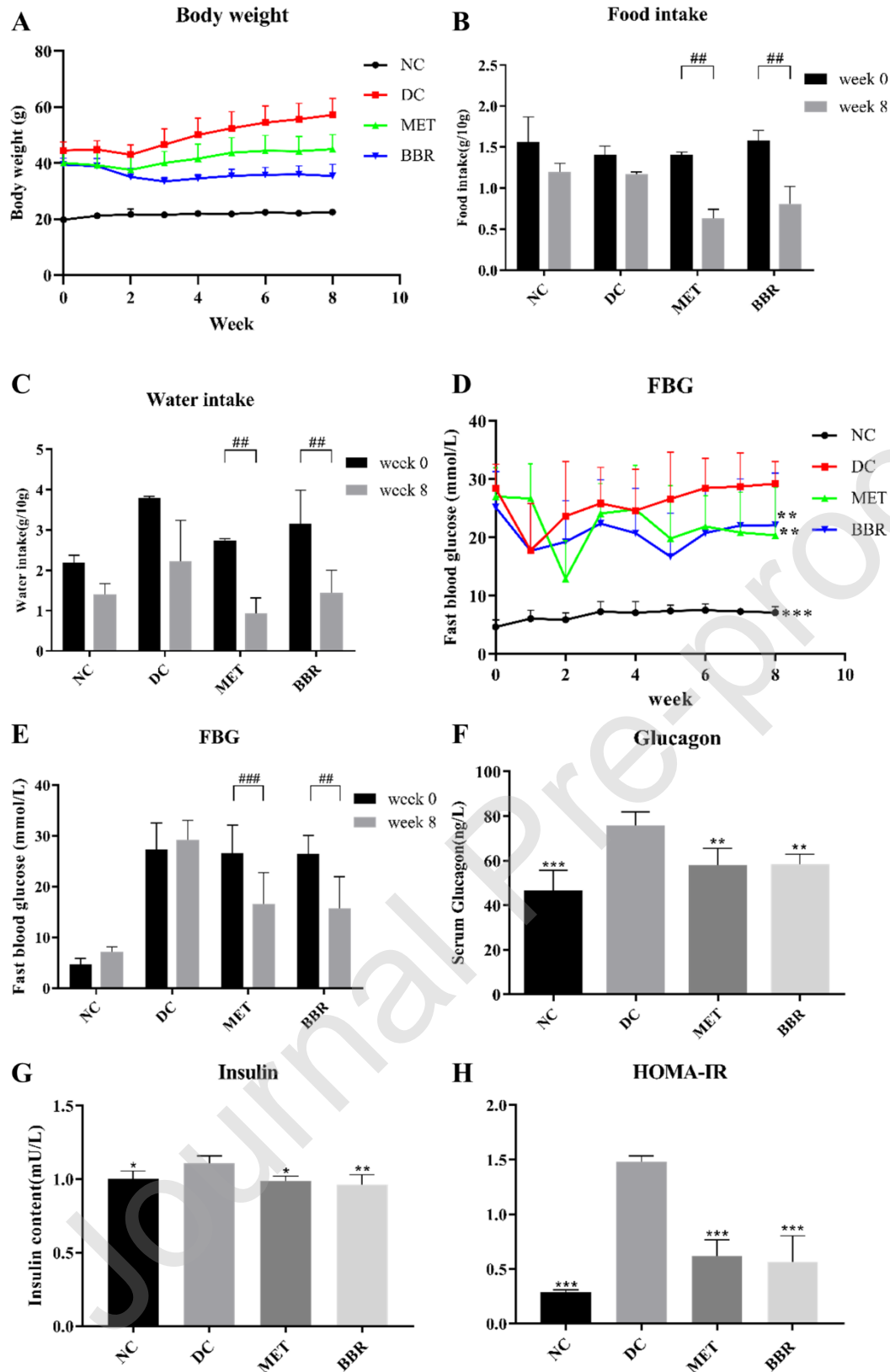


Fig. 1. Body weight (A), food intake over one day (B), water intake over one day (C), fasting blood glucose levels (D, E), glucagon level in serum (F), insulin content in serum (G) and

HOMA-IR (H) of each group. Data shown are mean \pm SD (n=10). ### $p < 0.001$, ## $p < 0.01$. *** $p < 0.001$, ** $p < 0.01$ vs. DC. * $p < 0.01$ vs. DC.

3.2. Effects of MET and BBR on key enzymes of glycogen metabolism in *db/db* mice

Both GP and GDBE are key enzymes in glycogen degradation: GP involves the (1 \rightarrow 4)- α glycosidic linkages, removing one unit at a time from the terminal end of a glycogen chain, while GDBE participates in the cleaving of (1 \rightarrow 6)- α glycosidic linkages, removing glycogen branch points (Adeva-Andany, Gonzalez-Lucan, Donapetry-Garcia, Fernandez-Fernandez & Ameneiros-Rodriguez, 2016). Under the combined action of GP and GDBE, glycogen molecules are degraded to supply glucose to meet physiological need. Therefore, the activity of GP and GDBE in liver tissue are closely related to the rate of enzymatic hydrolysis of glycogen. It has been reported that the activity of GP and GDBE are regulated by the level of serum glucagon (Liu et al., 2019). As shown in **Figs. 2A and B**, the activities of GP and GDBE in the liver tissue of diabetic mice were significantly higher than those in non-diabetic mice, which might be the result of the elevated glucagon levels in the *db/db* mice. The elevated activity of GP might result in faster levels of glycogen degradation. After treatment with MET and BBR, the activities of GP and GDBE in *db/db* mice were both significantly decreased. The combination of these data suggests that, thus both MET and BBR may inhibit glycogenolysis and reduce hepatic glucose production in diabetic mice through the regulation of GP via a reduction in glucagon.

MET and BBR may inhibit excessive gluconeogenesis (Madiraju et al., 2014; Zhang et al., 2018). Here, we measured the protein levels of G-6-Pase and PEPCK, which are the rate-

limiting enzymes in the gluconeogenesis process (Chung, Chacko, Sunehag & Haymond, 2015; Oh, Han, Kim & Koo, 2013). It can be seen in **Fig. 2C, D** that the activities of G-6-Pase and PEPCK were significantly increased in *db/db* mice compared with non-diabetic mice, while there was a statistically significant reduction in the activity of G-6-Pase and PEPCK in diabetic mice after MET and BBR treatment. The data displayed here are consistent with that previously reported (Liu et al., 2019).

Glycogenesis is the reverse of glycogen degradation. During glycogenesis, excess glucose is transferred into the liver, muscle and other tissues to be stored as glycogen. Glycogen synthesis is regulated by insulin levels and is important for maintaining blood-glucose homeostasis. Glycogen synthase (GS), the rate-limiting enzyme in the glycogenesis process, catalyses the formation of (1→4)- α glycosidic linkages, using UDP-glucose as a glucose donor, to a growing glycogen chain (Wang et al., 2018). As shown in **Fig. 2E**, the activity of GS in *db/db* mice was observed to be higher than in non-diabetic mice, indicating that glycogenesis was enhanced in *db/db* mice. The abnormal activity of GS in *db/db* mice might be caused by multiple factors, such as insulin resistance and the level of glucose 6-phosphate (G6P). When insulin resistance occurs, insulin secretion in the body will be increased, which in turn causes excessive activation of the phosphatidylinositol 3 kinase/protein kinase B/glycogen synthase 3 kinase (PI3K/AKT/GSK3 β) signaling pathway, resulting in increased GS activity (Wang et al., 2018). In addition, excessive blood glucose is transferred into liver under the state of hyperglycaemia, resulting in increased level of G6P (GS agonist), which further activates GS (Bouskila et al., 2010). After MET and BBR treatment, the activity of GS was significantly

decreased in *db/db* mice. From the data in **Fig. 1G, H**, MET and BBR can reduce the level of insulin, HOMA-IR and FBG in diabetic mice. Thus, MET and BBR decreased the activity of GS and regulated glycogenesis, possibly by regulating insulin level, and improving insulin resistance and hyperglycaemia.

Summarizing the above results, the activity of the main enzymes involved in glycogen synthesis and degradation was accelerated, and gluconeogenesis were enhanced in diabetic mice, with MET and BBR. Since GS, GP and GDBE are also involved in the formation of glycogen's structure, these changes to glycogen metabolism in diabetes may not only result in changes of glycogen content but also glycogen structure. MET and BBR may regulate the key enzymes in glycogen metabolism, such as GP, GDBE, GS, G-6-Pase and PEPCK, and thus improve glycogenolysis, glycogenesis and gluconeogenesis in diabetic mice.

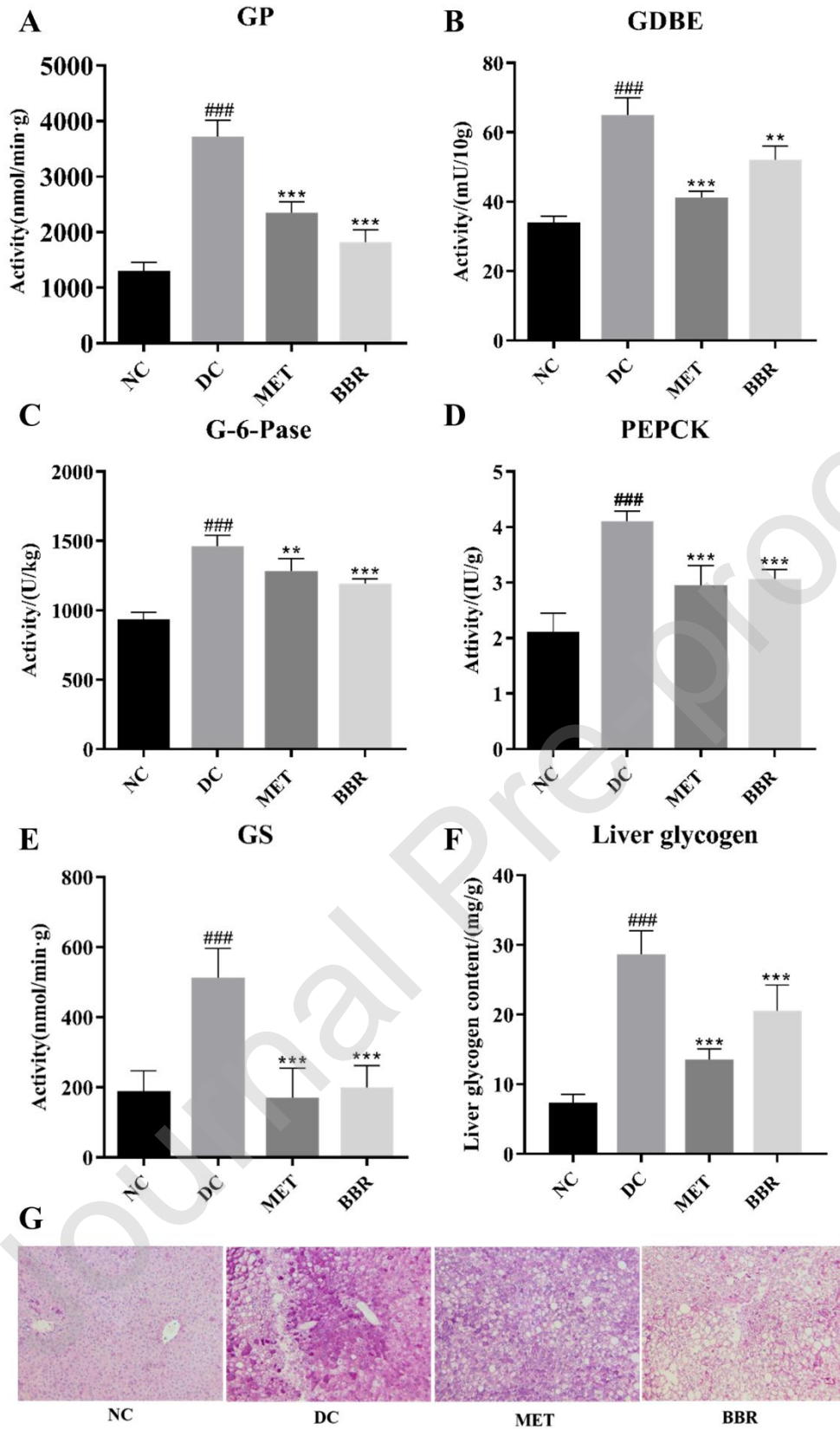


Fig. 2. The effects of MET and BBR on the enzymes of glycogen metabolism (A, B, C, D and E) and glycogen content (F and G). Data shown are mean \pm SD (n=6). ### $p < 0.001$ vs. NC. *** $p < 0.001$, ** $p < 0.01$ vs. DC.

3.3. Effects of MET and BBR on liver glycogen content

Although fasting the mice and the administration of anesthetics may cause some changes of liver glycogen content (Sullivan et al., 2014), all groups in this study had the same procedure, still allowing a meaningful comparison of the glycogen content of each group. The liver glycogen content is displayed in **Fig. 2F**. The liver glycogen content in diabetic mice was significantly higher than in non-diabetic mice, however after treatment with MET and BBR, the liver glycogen content markedly dropped. This is consistent with previous reports (Li et al., 2019). PAS staining reflected glycogen accumulation and distribution in liver tissues (**Fig. 2G**). As shown in **Fig. 2G**, the staining colour in the DC group was more intense than in the NC group, which indicates that excess glycogen accumulated in the livers of *db/db* mice. However, after MET and BBR treatment, the liver glycogen accumulation in *db/db* mice was decreased. The PAS staining images were consistent to the liver glycogen content assay results. As the results show above, glycogenolysis was elevated because of the increased activity of GP in *db/db* mice. At first sight, it would be expected that the glycogen content in *db/db* mice should be lower than that in healthy mice, but the result is the opposite. The higher liver glycogen content in *db/db* mice might be a result of the abnormally elevated activity of GS. After MET and BBR treatment, the liver glycogen content was decreased in *db/db* mice. The change of

liver glycogen content was consistent with the change in GS activity, which indicated that the activity of GS may be determining the liver glycogen content.

3.4. Effects of MET and BBR on glycogenolysis via cAMP/PKA signaling pathways

In liver tissues, the cAMP/PKA pathway is the major upstream signaling pathway of GP. It is triggered by the combination of glucagon to its Gs-coupled receptors (GPCR), which could further activate the membrane-bound adenylyl cyclase (AC). Intracellular cAMP is a type of second messenger, which is converted from adenosine triphosphate (ATP) through the catalysis of activated membrane-bound AC (Paramonov, Mamaeva, Sahlgren & Rivero-Muller, 2015). The increased intracellular levels of cAMP could act as the upstream kinase for cAMP-dependent protein kinase A (PKA), and then stimulate the activation of glycogen phosphorylase kinase (PK). PK is a serine/threonine-specific protein kinase which converts GP_b to GP_a. The active state of PK is when it is phosphorylated (p-PK) (Yang & Yang, 2016). Finally, this GP_a begins the process of glycogenolysis. Under diabetic conditions, however, the excessive glucagon levels would over-activate the cAMP/PKA signaling pathway and accelerate the degradation of glycogen.

The ELISA quantification of cAMP content and the western blot analysis of GPCR, PKA, PK, p-PK and GP_a in liver tissue are displayed in **Fig. 3**. As mentioned above, the level of glucagon in the serum of *db/db* mice was significantly higher than that of healthy mice, which could increase the amount of glucagon binding to the GPCR. It can be seen in **Fig. 3** that the expression of GPCR and the content of cAMP in the livers of *db/db* mice were substantially higher than that of non-diabetic mice. Consequently, the levels of PKA, PK, p-PK and GP_a in

the livers of *db/db* mice were significantly higher than in non-diabetic mice. Excessive glucagon in the serum of diabetic mice could lead to the excessive activation of GP α through a series of reactions mentioned above. However, after treatment with MET and BBR, the content of cAMP and the expression level of GPCR, PKA, PK, p-PK and GP α were markedly decreased, as hypothesized. These results indicate that MET and BBR might inhibit the conversion of GP β to GP α and restrain the degradation of glycogen via the cAMP/PKA signaling pathway.

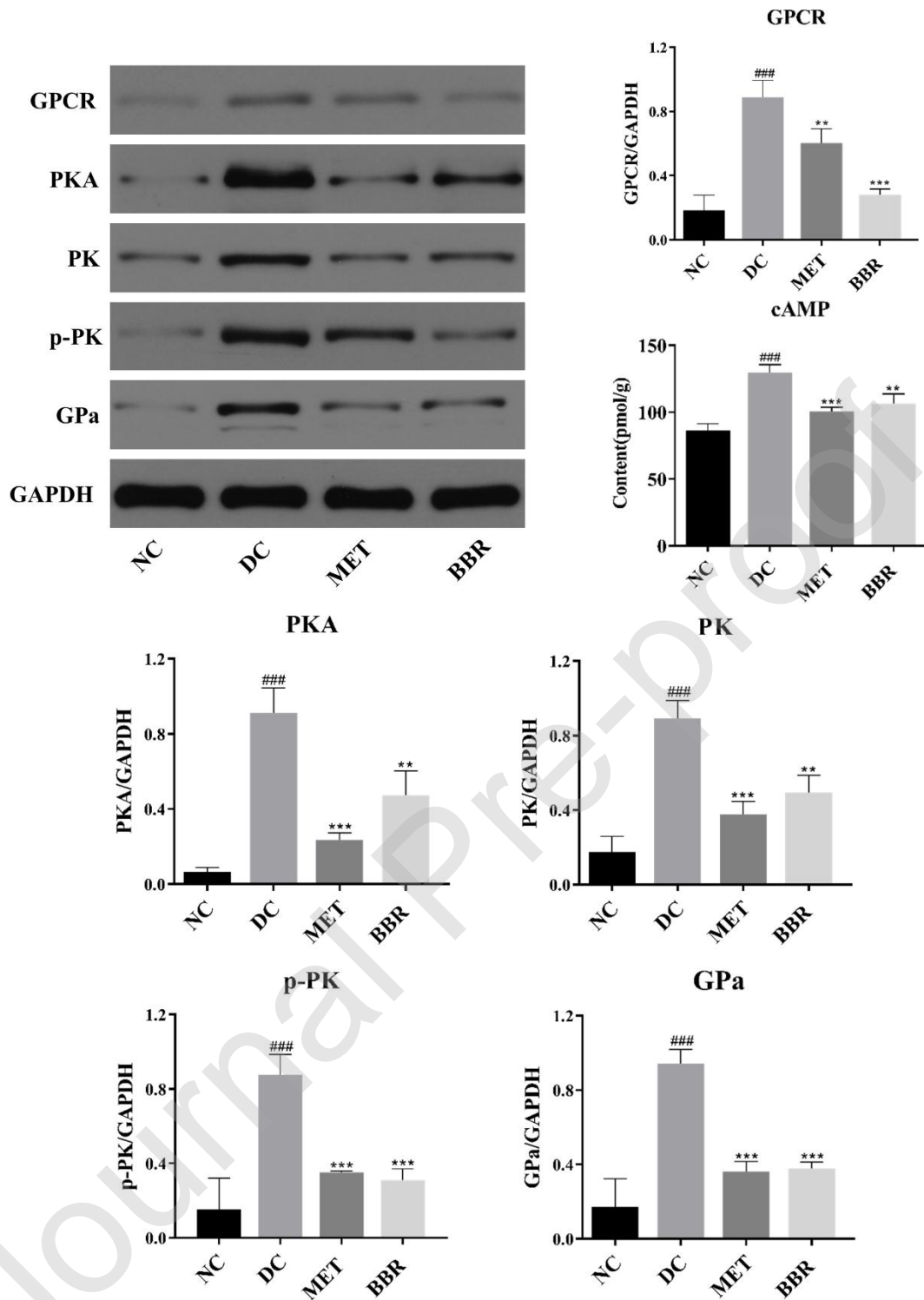


Fig. 3. The effects of MET and BBR on the glycogenolysis pathway in *db/db* mice. Data shown are mean \pm SD (n=3). ### $p < 0.001$ vs. NC. *** $p < 0.001$, ** $p < 0.01$ vs. DC.

3.5. Effects of MET and BBR on gluconeogenesis via AMPK/HNF-4 α signaling pathways

Glucose-6-phosphatase (G-6-Pase) and phosphoenolpyruvate carboxykinase (PEPCK) are two key enzymes in gluconeogenesis. PEPCK simultaneously decarboxylates and phosphorylates oxaloacetate into phosphoenolpyruvate, one of the earliest, rate-limiting steps in gluconeogenesis, and G-6-Pase catalyzes the final step in both gluconeogenic and glycogenolytic pathways (Liu et al., 2019). The hepatocyte nuclear factor-4 α (HNF-4 α) and AMP-activated protein kinase (AMPK) are two important upstream regulatory proteins for G-6-Pase and PEPCK. HNF-4 α can promote the expression of G-6-Pase and PEPCK via binding to cis-elements in their promoters (Wei et al., 2016), and p-AMPK, as an active form of AMPK, can restrain the transcriptional activity of the cAMP-responsive element (CRE) to down-regulate the expression of G-6-Pase and PEPCK (Zhang, Chen, Zeng, Huang & Xu, 2019). As presented in **Fig. 4**, the expressions of G-6-Pase and PEPCK in diabetic livers were much higher than in non-diabetic livers, which indicate that gluconeogenesis was enhanced in *db/db* mice. After treatment with MET and BBR, the expression of G-6-Pase, PEPCK and HNF-4 α were significantly decreased, the expression of total AMPK was not significantly changed among the four groups, while the expression of p-AMPK and the ratio of p-AMPK/AMPK were increased. This result indicates that MET and BBR might decrease the expression of G-6-Pase and PEPCK by regulation of HNF-4 α and p-AMPK.

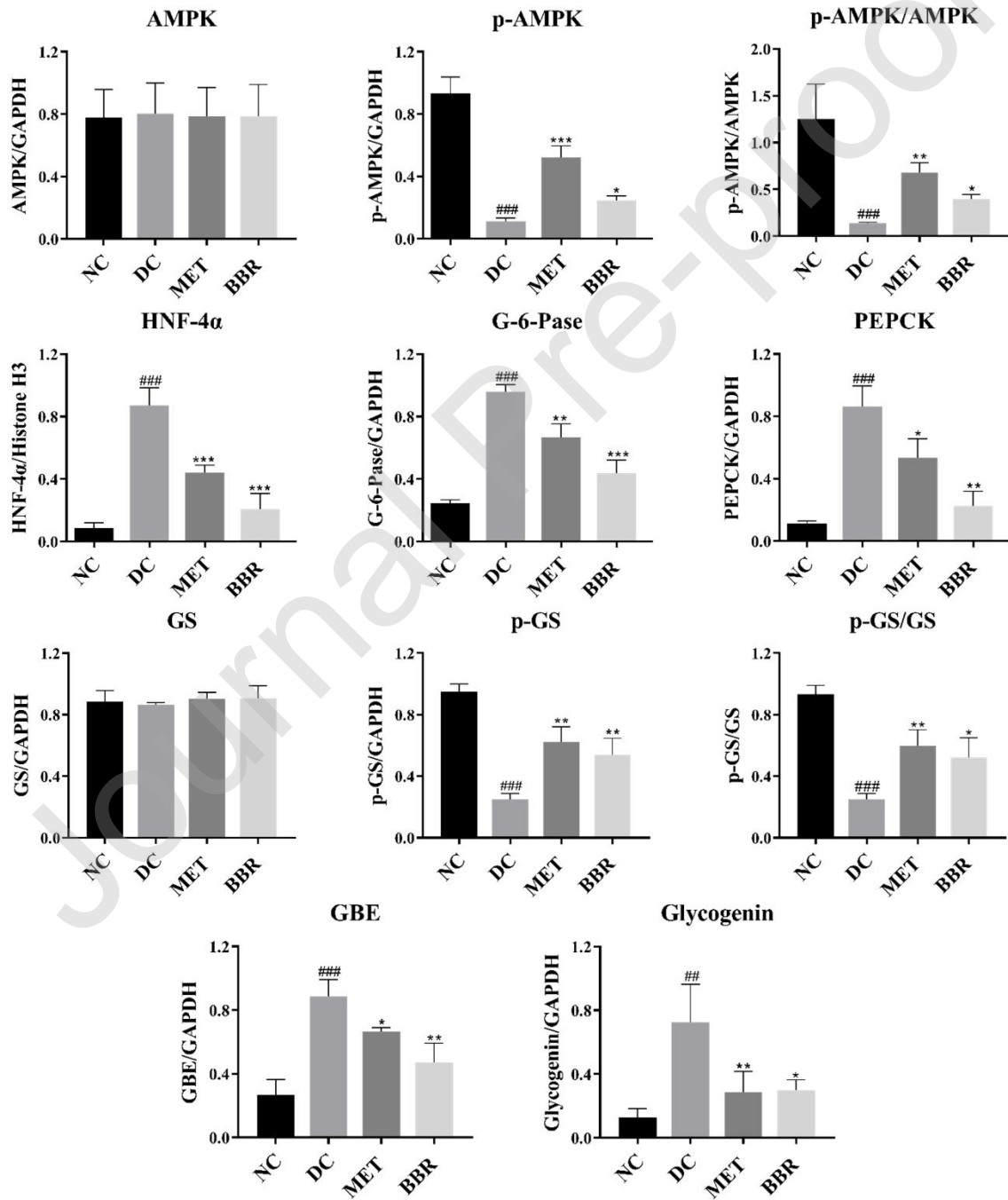
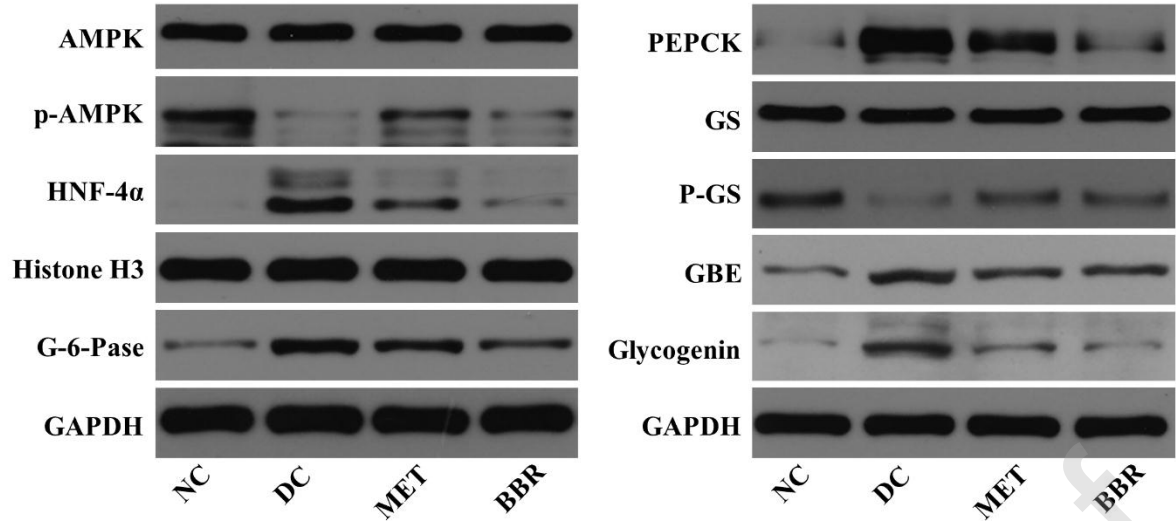


Fig. 4. The effects of MET and BBR on the pathways involved in gluconeogenesis and glycogenesis in *db/db* mice. Data shown are mean \pm SD (n=3). ### $p < 0.001$, ## $p < 0.01$ vs. NC.

*** $p < 0.001$, ** $p < 0.01$, * $p < 0.05$ vs. DC.

3.6. Effects of MET and BBR on glycogenesis via AMPK/GS signaling pathways

Glycogenin, GS and glycogen branching enzyme (GBE) are three important enzymes involved in the process of glycogen synthesis. Glycogenin is the initial enzyme in glycogen polymerization; forming the centre of a growing glycogen molecule and attaching the initial glucose molecules to itself, using UDP-glucose as the substrate (Tan, Sullivan, Nada, Deng, Schulz & Gilbert, 2018). GS adds new glucose molecules to the non-reducing end of original glycogen via (1 \rightarrow 4)- α glycosidic bonds, again using UDP-glucose as the glucose donor. GBE adds branches to glycogen molecules via (1 \rightarrow 6)- α glycosidic bonds. GS catalyses the formation of the linear chains of glycogen, while GBE catalyses the formation of branches of glycogen (Liu et al., 2019). Among these three enzymes, GS is the rate-limiting enzyme in glycogen synthesis. In addition to allosteric regulation, GS is also regulated by phosphorylation and dephosphorylation leading to deactivation and activation, respectively. GS activation may therefore take place through inactivation of GS kinases and by activation of GS phosphatases. It has been demonstrated that AMPK, as a GS kinase, can phosphorylate the site 2 located near the N-terminus of GS (p-GS, inactive state of GS) and thus decrease the activity of GS (Wojtaszewski, Nielsen, Jørgensen, Frøsig, Birk & Richter).

To explore the effects of MET and BBR on glycogen synthesis and its upstream pathway, the expression levels of glycogenin, GS, p-GS, GBE, AMPK and p-AMPK were measured and

are presented in **Fig. 4**. The expression levels of total GS among four groups didn't show significant difference, but the expression level of p-GS and the ratio of p-GS/GS were obviously decreased in diabetic mice, the lower ratio of p-GS/GS meant the higher activation level of GS. Moreover, the expression level of glycogenin and GBE in *db/db* mice were significantly higher than those of non-diabetic mice. This indicates that glycogenesis was abnormally enhanced in *db/db* mice. However, the expression levels of p-GS, glycogenin, GBE and the ratio of p-GS/GS in diabetic mice were reversed after MET and BBR treatment, which suggested that MET and BBR could improve glycogenesis by inhibiting GS, GBE and glycogenin. The result here is consistent with the data for GS activity and glycogen content presented above. The expression level of total AMPK was similar among the four groups, while the expression of p-AMPK (the active state of AMPK) and the ratio of p-AMPK/AMPK in *db/db* mice were lower than in non-diabetic mice. Moreover, the expression of p-AMPK and the ratio of p-AMPK/AMPK in *db/db* mice were increased after treatment with MET and BBR. These data indicated that MET and BBR could reduce glycogenesis by potentially activating AMPK and thus inhibiting GS (the rate-limiting enzyme in glycogenesis).

3.7. Effects of MET and BBR on glycogen molecular weight distributions in *db/db* mice

The SEC weight distributions as a function of molecular size for glycogen particles from the four groups are shown in **Fig. 5**, normalized to their maxima. The blue and red lines represent untreated and DMSO treated glycogen, respectively. DMSO treatment is an efficient way to test the stability of glycogen particles. The change of size distributions before and after DMSO treatment shows the stability of glycogen particles. As expected from previous studies

(Deng et al., 2015), untreated glycogen from NC and DC group had similar size distributions, consisting of a significant population of α particles. However, after DMSO treatment, most glycogen particles in the DC group were degraded into smaller particles, with the main peak changing to 18 nm (corresponding to β particles). This is consistent with our previous study that liver glycogen in *db/db* mice is fragile and easily degraded into smaller particles (Deng et al., 2015). However, the size distributions of glycogen from MET and BBR groups did not undergo this large change after DMSO treatment. Here the main peak remained at ~ 40 nm, corresponding to α particles. This indicated that glycogen α particles from MET and BBR treated groups were more stable compared with *db/db* mice after DMSO treatment.

To quantify the extent of degradation of α particles from each group, the average R_h values before and after DMSO treatment and the degradation quotient were calculated and are shown in **Table 1**. The degradation quotient was calculated as the ratio of the initial R_h of the untreated sample, to that after DMSO treatment. The higher the degradation quotient, the greater the extent of degradation under DMSO treatment. The average R_h of diabetic liver glycogen was 28 ± 6 nm and was dramatically reduced to 20 ± 2 nm after DMSO treatment, indicating that particles were significantly degraded. Small reductions of the average R_h were observed in DMSO-treated glycogen from NC, MET and BBR groups, but there were no statistically significant differences of the average R_h in these three groups before and after treatment. It can be seen in **Table 1** that the glycogen in DC group had a higher degradation quotient (1.4 ± 0.2) compared to that in NC group (1.1 ± 0.1), which means more degradation occurred in the glycogen of *db/db* mice. The degradation quotients in MET and BBR groups were significantly

decreased to 1.1 ± 0.2 and 1.1 ± 0.2 , respectively, resembling the NC group. All these data suggested MET and BBR could strengthen the fragile liver α particles in diabetic mice.

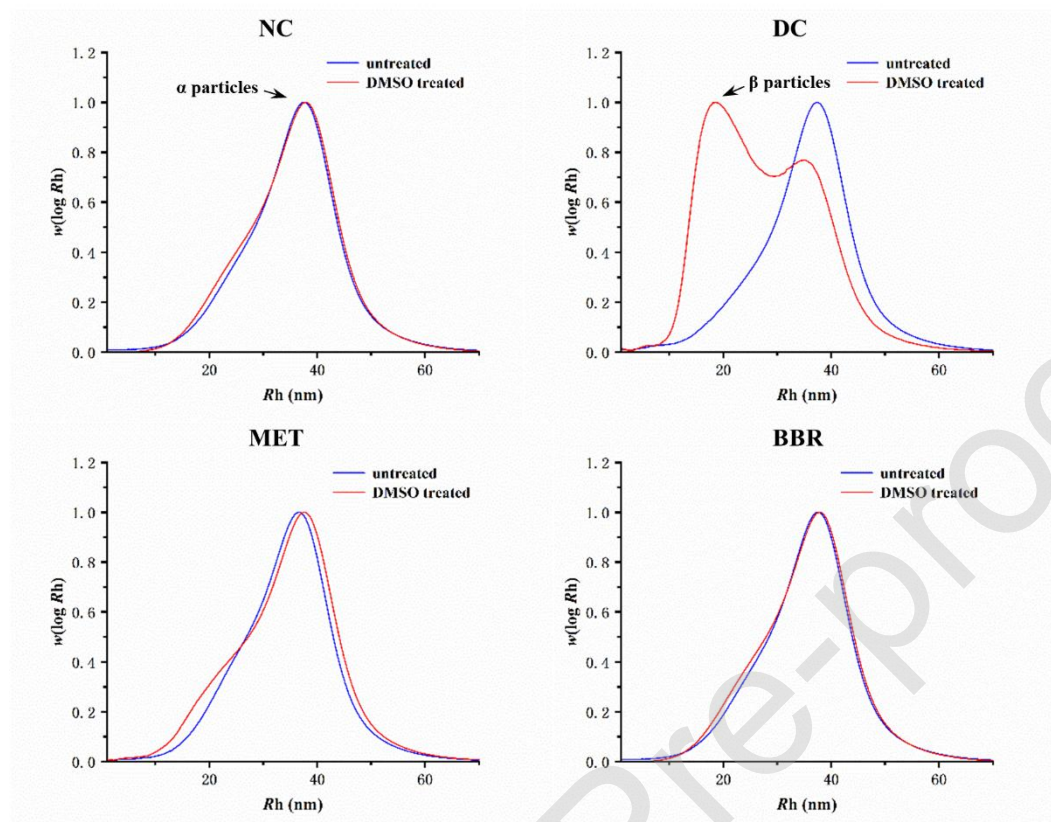


Fig. 5. The glycogen SEC weight distributions of each group before and after DMSO treated (n=6). A representative sample for each group is shown here, with all samples given in supplementary information.

Table 1. The average R_h of untreated and DMSO treated glycogen and degradation quotient from SEC data of each group (n=6).

Group	Average R_h (nm)		Degradation quotient
	untreated	DMSO treated	
NC	23.7 ± 2.9	21.6 ± 1.7	1.1 ± 0.1

DC	27.6±6.0	20.3±1.8 ^{##}	1.4±0.2 [#]
MET	25.7±3.8	23.5±1.2	1.1±0.2*
BBR	25.1±4.1	23.7±2.7	1.1±0.0*

Data shown are mean \pm SD. ^{##} $p < 0.01$ vs. untreated. [#] $p < 0.05$ vs. NC. * $p < 0.05$ vs. DC.

3.8. Effects of MET and BBR on glycogen density distributions in *db/db* mice

The molecular density distributions and average density values of glycogen from the four groups are shown in **Fig. 6**. The average values were calculated over an R_h range from 20~55 nm. The average density was calculated as previously reported, as $\int \rho(R_h) dR_h / (R_{h,max} - R_{h,min})$ (Hu et al., 2018). The R_h ranges for these distributions were chosen to have acceptable signal: noise ratios, these ranges differing for the DRI and MALLS detectors. The MALLS detector has poorer signal: noise at a lower R_h and can produce signal noise artifacts at these sizes. As expected from a previous study (Hu et al., 2019), *db/db* mouse liver glycogen had a higher molecular density than non-diabetic mice, but had a substantial density reduction after DMSO treatment. This is probably caused by a loss of some component associated with glycogen, due to hydrogen bonds being broken in protein-oligosaccharides association (Tan, Sullivan, Nada, Deng, Schulz & Gilbert, 2018). Fragile α particles were broken apart into β particles, which had a smaller density than α particles. However, no density decrease was observed in glycogen from MET and BBR group. This also indicates MET and BBR could convert fragile α particles into the stable state in glycogen of *db/db* mice.

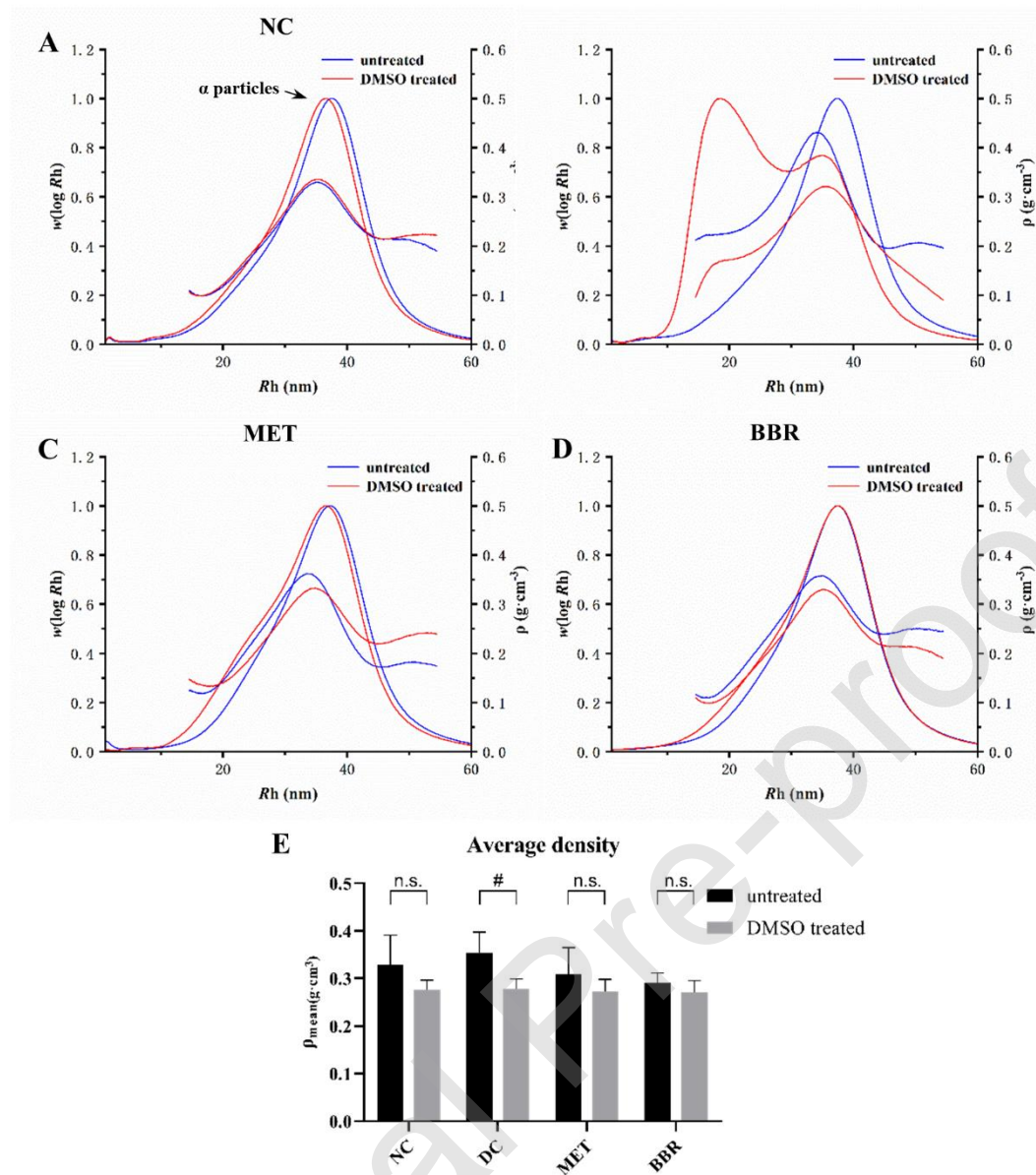


Fig. 6. The analysis of glycogen density distribution of each group before and after DMSO treated. A representative sample for each group is shown with all samples given in supplementary information. Data shown are mean \pm SD (n=6). # $p < 0.05$. n.s. $p > 0.05$ (n.s. means no significant difference).

3.9. Transmission electron microscopy analysis of liver glycogen

The TEM images of glycogen treated with DMSO are presented in **Fig. 7**. After DMSO treatment, the glycogen from non-diabetic liver mainly comprised α particles, which have the

appearance of cauliflower. Conversely, the glycogen from diabetic liver was more likely to degrade into β particles. However, liver glycogen from MET and BBR groups mostly maintained its compact α -particle structure with only a few β particles. This result suggests that MET and BBR could improve the fragility to DMSO of glycogen in *db/db* mice, which is consistent with the inference from SEC data.

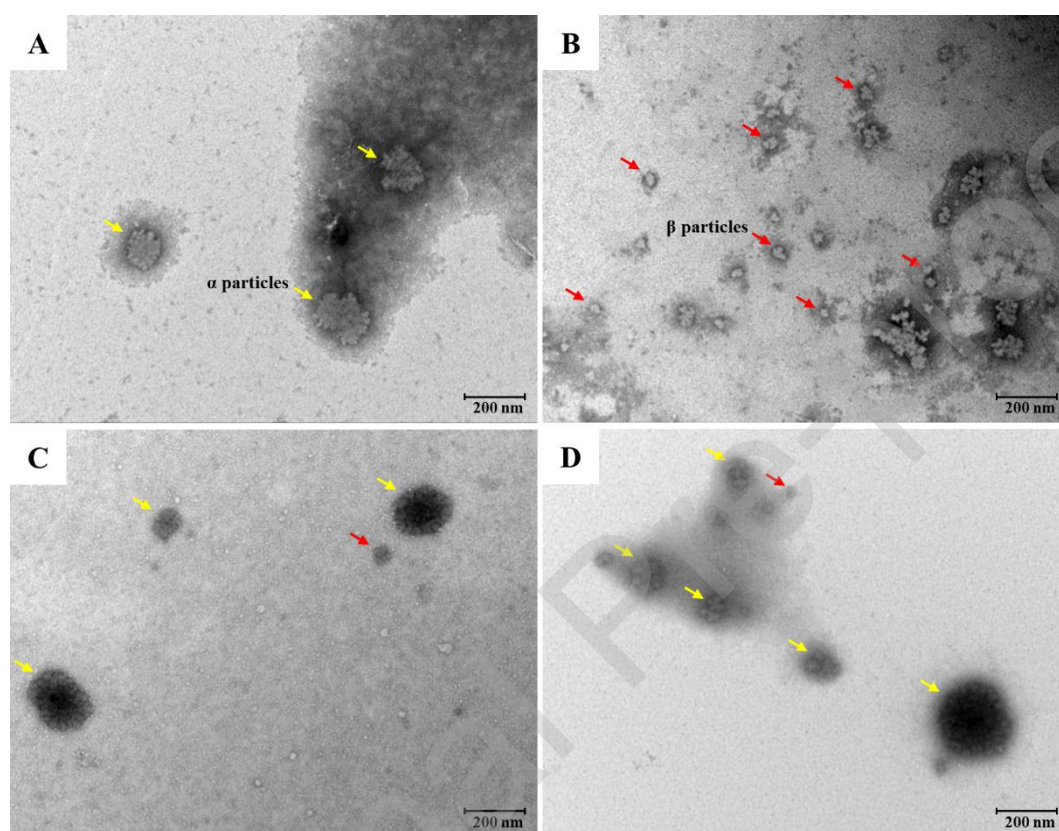


Fig. 7. TEM micrograph of liver glycogen after DMSO treatment. (A) NC group; (B) DC group; (C) MET group; (D) BBR group.

3.10. Effects of MET and BBR on the chain-length distributions

The CLDs, as functions of the degree of polymerization of chains, were measured by a standard method, using isoamylase to break all (1 \rightarrow 6)- α branch points enzymatically, followed by quantification of the abundance of each resulting chain length by FACE. The FACE

electrophorogram, CLD, average chain length (ACL) and degree of branching are given in **Fig. 8**. The distributions of DC group are consistent with those of glycogen from a previous study (Hu et al., 2018), with glycogen from diabetic mice having a higher proportion of longer chains, larger ACL and lower degree of branching.

Potentially these longer chain lengths and fewer branch points could contribute to the molecular fragility seen in diabetic liver glycogen. In the present study, the CLDs of MET and BBR group are similar to those from NC group, compared to that of the DC group. The ACL of these two groups were decreased and the degree of branching of these two groups were elevated, compared to the DC group, resembling the non-diabetic group. These data show that MET and BBR could change the CLD of glycogen in diabetic mice to that healthy glycogen, and also indicates that changing the CLD might be the underlying mechanism of MET and BBR repairing the impaired structure of liver glycogen.

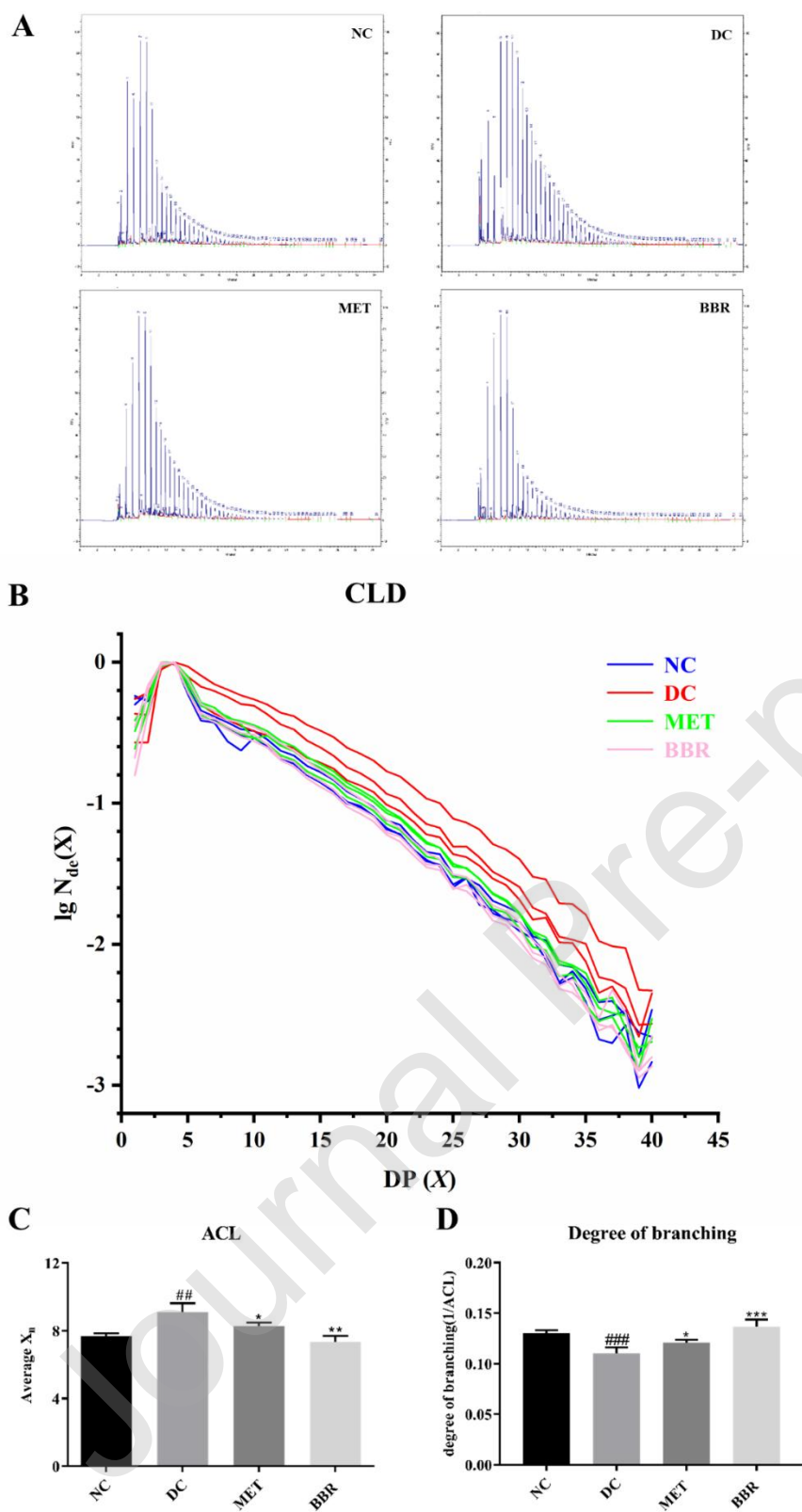


Fig. 8. Examples of FACE electrophoretograms (A), the chain-length distribution (B), the average degree of polymerization (C) and the degree of branching (D) of glycogen from each

group. Data shown are mean \pm SD (n=3). ### $p<0.001$, ## $p<0.01$ vs. NC. *** $p<0.001$, ** $p<0.01$, * $p<0.05$ vs. DC.

3.11. Effects of MET and BBR on the affinity of GP with glycogen from *db/db* mice *in vitro*

The Michaelis constant (K_m) expresses the concentration of the substrate at half of the maximum velocity (V_{max}) of the reaction (Milne et al., 2007; Schnell, 2014). The lower the K_m value, the higher the affinity of the enzyme to the substrate (Michaelis, Menten, Johnson & Goody, 2011).

The reaction rate profiles and Lineweaver-Burk profiles are given in **Fig. 9**. The K_m values were calculated through Lineweaver-Burk profile and the formula $1/v = K_m/(V_{max}[S]) + 1/V_{max}$ (v =the reaction rate, V_{max} = the maximum velocity). The K_m value of glycogen to GP of NC, DC, MET and BBR groups were 1.1 ± 0.2 , 0.49 ± 0.15 , 0.90 ± 0.11 and 0.82 ± 0.14 mg/mL, respectively. As presented in **Fig. 9**, for a given substrate (glycogen) concentration, the reaction velocity of the DC group is much higher than the other three groups, and the K_m value is smaller than for non-diabetic glycogen. This indicates that glycogen from diabetic mice has a stronger affinity with GP than healthy glycogen. This stronger affinity might be attributed to the longer chains and loose structure in glycogen molecules in diabetic mice, which could be easier to attach to the GP bonding sites and therefore be degraded. After the intervention of MET and BBR, the reaction velocity at the same concentration of glycogen from *db/db* mice decreased dramatically and the K_m value of glycogen to GP was substantially increased. This might be the result of the more stable molecular structure of glycogen in *db/db* mice after the treatment with MET and BBR. All these data here indicate that modifying impaired glycogen structure could

weaken the affinity of glycogen to GP and decrease the degradation rate, which might be the mechanism of MET and BBR inhibiting glycogenolysis.

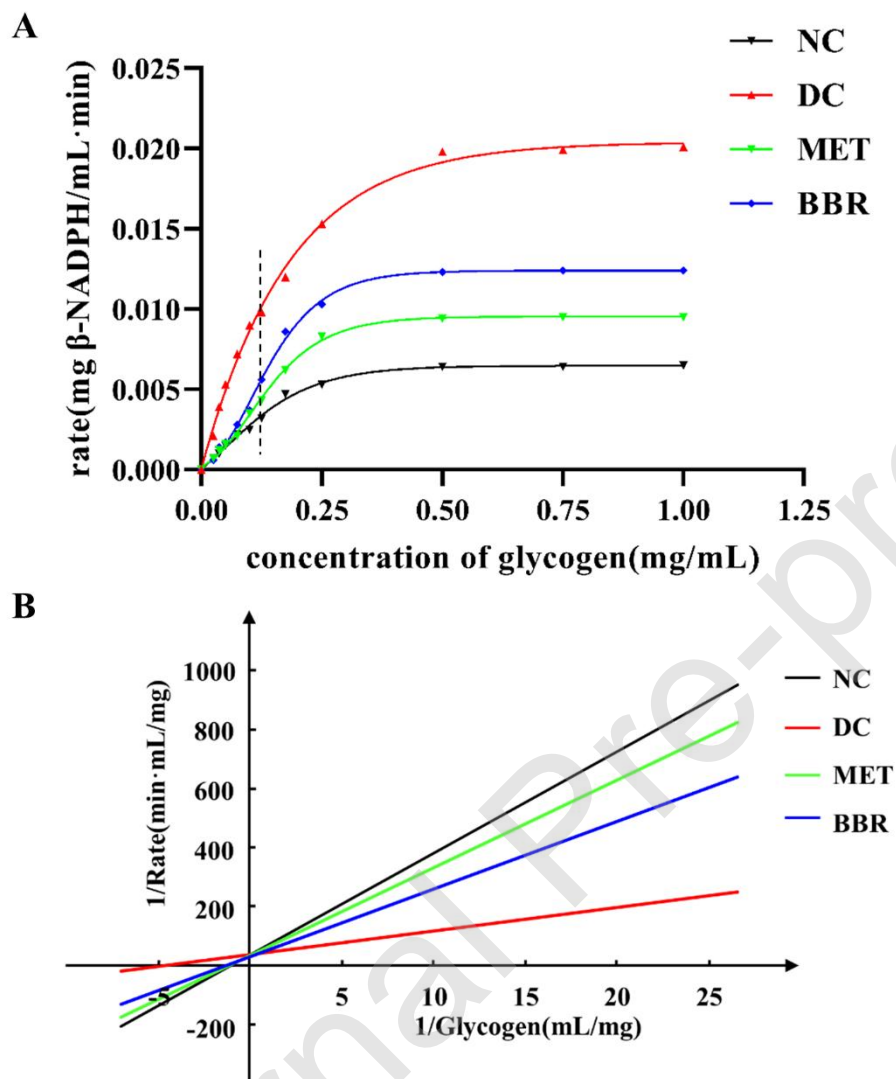


Fig. 9. The assay of the affinity of GP with the glycogen from each group. Reaction rate profile for GP with a series of concentrations of glycogen (A). Lineweaver-Burk profile with double-reciprocal plot for GP enzymatic reaction at a series of concentrations of glycogen (B). A representative sample for each group is shown with all samples given in supplementary information (n=3).

4. Conclusion

This paper studied how key aspects of glycogen metabolism and glycogen structure from *db/db* mice were affected by the treatment of two anti-diabetic drugs, MET and BBR. Our results indicate that MET and BBR down-regulate the cAMP/PKA signaling pathway to inhibit the expression of GP α , thus inhibiting the excessive glycogenolysis presented in diabetic livers, a major contributor to the abnormal blood glucose levels seen in diabetes. MET and BBR also appears to repair the altered glycogen structure seen in *db/db* mice to that in healthy, with the α particles becoming more stable and the chain lengths, degree of branching and molecular density resembling non-diabetic glycogen. The repair of glycogen structure might be a reason that MET and BBR weaken the affinity of glycogen to GP in *db/db* mice back to non-diabetic levels. This decreased affinity of glycogen to GP could slow down the rate of glycogenolysis, thus inhibiting the excessive hepatic glucose output seen in diabetes. In addition, MET and BBR could inhibit gluconeogenesis in diabetic liver via the AMPK/HNF-4 α pathway and inhibit the glycogenesis through the AMPK/GS signaling pathway in *db/db* mice. These effects of MET and BBR mentioned above could effectively down-regulate hepatic glucose output by inhibiting both glycogenolysis and gluconeogenesis. Since abnormal hepatic glucose output is a characteristic manifestation of diabetes, this increased understanding of the mechanisms by which MET and BBR suppress hepatic glucose output may provide new targets for the development of novel anti-diabetic drugs.

CRedit author statement

Xiaocui Liu: Investigation, Writing - Original Draft

Kaiping Wang: Investigation, Project administration

Jing Zhou: Validation

Mitchell A. Sullivan: Writing-Review & Editing

Yage Liu: Investigation

Robert G. Gilbert: Supervision

Bin Deng: Conceptualization, Funding acquisition, Supervision

Declaration of competing interest

The authors declare no conflicts of interest.

Acknowledgements

This work was supported by the National Natural Science Foundation of China (Grants No.81803799 and C1304013151101138). The support of the Fundamental Research Funds for the Central Universities (2017KFYXJJ252) and the 1000-Talents Program of the Chinese State Administration of the Foreign Experts Bureau are also gratefully acknowledged. M.A.S. is supported by a Mater Research McGuckin Early Career Fellowship, the University of Queensland's Amplify Initiative and Mater Foundation. A project funded by the Priority Academic Program of Jiangsu Higher Education Institutions.

References

Adeva-Andany, M. M., Gonzalez-Lucan, M., Donapetry-Garcia, C., Fernandez-Fernandez, C., & Ameneiros-Rodriguez, E. (2016). Glycogen metabolism in humans. *BBA Clin*, 5, 85-100.

- Agius, L. (2015). Role of glycogen phosphorylase in liver glycogen metabolism. *Mol Aspects Med*, 46, 34-45.
- Balbaa, M., El-Zeftawy, M., Ghareeb, D., Taha, N., & Mandour, A. W. (2016). Nigella sativa Relieves the Altered Insulin Receptor Signaling in Streptozotocin-Induced Diabetic Rats Fed with a High-Fat Diet. *Oxid Med Cell Longev*, 2016, 2492107.
- Bao, F., Yang, K., Wu, C., Gao, S., Wang, P., Chen, L., & Li, H. (2018). New natural inhibitors of hexokinase 2 (HK2): Steroids from Ganoderma sinense. *Fitoterapia*, 125, 123-129.
- Barr, D., Szennyes, E., Bokor, E., Al-Oanzi, Z. H., Moffatt, C., Kun, S., Docsa, T., Sipos, A., Davies, M. P., Mathomes, R. T., Snape, T. J., Agius, L., Somsak, L., & Hayes, J. M. (2019). Identification of C-beta-d-Glucopyranosyl Azole-Type Inhibitors of Glycogen Phosphorylase That Reduce Glycogenolysis in Hepatocytes: In Silico Design, Synthesis, in Vitro Kinetics, and ex Vivo Studies. *ACS Chem Biol*, 14(7), 1460-1470.
- Boden, G. (2004). Gluconeogenesis and glycogenolysis in health and diabetes. *J Investig Med*, 52(6), 375-378.
- Bouskila, M., Hunter, R. W., Ibrahim, A. F., Delattre, L., Peggie, M., van Diepen, J. A., Voshol, P. J., Jensen, J., & Sakamoto, K. (2010). Allosteric regulation of glycogen synthase controls glycogen synthesis in muscle. *Cell Metab*, 12(5), 456-466.
- Chang, W., Chen, L., & Hatch, G. M. (2015). Berberine as a therapy for type 2 diabetes and its complications: From mechanism of action to clinical studies. *Biochem Cell Biol*, 93(5), 479-486.
- Chung, S. T., Chacko, S. K., Sunehag, A. L., & Haymond, M. W. (2015). Measurements of Gluconeogenesis and Glycogenolysis: A Methodological Review. *Diabetes*, 64(12), 3996-4010.
- Deng, B., Sullivan, M. A., Chen, C., Li, J., Powell, P. O., Hu, Z., & Gilbert, R. G. (2016). Molecular Structure of Human-Liver Glycogen. *PLoS One*, 11(3), e0150540.
- Deng, B., Sullivan, M. A., Li, J., Tan, X., Zhu, C., Schulz, B. L., & Gilbert, R. G. (2015). Molecular structure of glycogen in diabetic liver. *Glycoconj J*, 32(3-4), 113-118.

- Duran, J., Gruart, A., Varea, O., Lopez-Soldado, I., Delgado-Garcia, J. M., & Guinovart, J. J. (2019). Lack of Neuronal Glycogen Impairs Memory Formation and Learning-Dependent Synaptic Plasticity in Mice. *Front Cell Neurosci*, *13*, 374.
- Ellingwood, S. S., & Cheng, A. (2018). Biochemical and clinical aspects of glycogen storage diseases. *J Endocrinol*, *238*(3), R131-R141.
- Girard, J. (2017). Glucagon, a key factor in the pathophysiology of type 2 diabetes. *Biochimie*, *143*, 33-36.
- Hansen, A. P., & Johansen, K. J. D. (1970). Diurnal patterns of blood glucose, serum free fatty acids, insulin, glucagon and growth hormone in normal and juvenile diabetics. *6*(1), 27-33.
- Hu, Z., Deng, B., Tan, X., Gan, H., Li, C., Nada, S. S., Sullivan, M. A., Li, J., Jiang, X., Li, E., & Gilbert, R. G. (2018). Diurnal changes of glycogen molecular structure in healthy and diabetic mice. *Carbohydr Polym*, *185*, 145-152.
- Hu, Z., Li, E., Sullivan, M. A., Tan, X., Deng, B., Gilbert, R. G., & Li, C. (2019). Glycogen structure in type 1 diabetic mice: Towards understanding the origin of diabetic glycogen molecular fragility. *Int J Biol Macromol*, *128*, 665-672.
- Hu, Z., Tan, X., Deng, B., Gan, H., Jiang, X., Wang, K., Li, C., Li, E., Gilbert, R. G., & Sullivan, M. A. (2017). Implications for biological function of lobe dependence of the molecular structure of liver glycogen. *European Polymer Journal*, *90*, 105-113.
- International, D. F. (2019). IDF Diabetes Atlas : 9th edn. Brussels, Belgium: 2019. Available at: <http://www.diabetesatlas.org>.
- Jayanthy, G., & Subramanian, S. (2014). Rosmarinic acid, a polyphenol, ameliorates hyperglycemia by regulating the key enzymes of carbohydrate metabolism in high fat diet – STZ induced experimental diabetes mellitus. *Biomedicine & Preventive Nutrition*, *4*(3), 431-437.
- Jiang, X., Zhang, P., Li, S., Tan, X., Hu, Z., Deng, B., Wang, K., Li, C., Sullivan, M. A., Li, E., & Gilbert, R. G. (2016). Molecular-size dependence of glycogen enzymatic degradation and its importance for diabetes. *European Polymer Journal*, *82*, 175-180.

- Klinov, S. V., & Kurganov, B. I. (2001). Kinetic mechanism of allosteric regulation of muscle glycogen phosphorylase B by adenosine 5'-monophosphate. *Biochemistry (Mosc)*, *66*(12), 1374-1377.
- Li, C., Gan, H., Tan, X., Hu, Z., Deng, B., Sullivan, M. A., & Gilbert, R. G. (2019). Effects of active ingredients from traditional Chinese medicines on glycogen molecular structure in diabetic mice. *European Polymer Journal*, *112*, 67-72.
- Liu, M. J., Wang, Z., Li, H. X., Wu, R. C., Liu, Y. Z., & Wu, Q. Y. (2004). Mitochondrial dysfunction as an early event in the process of apoptosis induced by woodfordin I in human leukemia K562 cells. *Toxicol Appl Pharmacol*, *194*(2), 141-155.
- Liu, Y., Yang, L., Zhang, Y., Liu, X., Wu, Z., Gilbert, R. G., Deng, B., & Wang, K. (2019). Dendrobium officinale polysaccharide ameliorates diabetic hepatic glucose metabolism via glucagon-mediated signaling pathways and modifying liver-glycogen structure. *J Ethnopharmacol*, *248*, 112308.
- Madiraju, A. K., Erion, D. M., Rahimi, Y., Zhang, X. M., Braddock, D. T., Albright, R. A., Prigaro, B. J., Wood, J. L., Bhanot, S., MacDonald, M. J., Jurczak, M. J., Camporez, J. P., Lee, H. Y., Cline, G. W., Samuel, V. T., Kibbey, R. G., & Shulman, G. I. (2014). Metformin suppresses gluconeogenesis by inhibiting mitochondrial glycerophosphate dehydrogenase. *Nature*, *510*(7506), 542-546.
- Michaelis, L., Menten, M. L., Johnson, K. A., & Goody, R. S. (2011). The original Michaelis constant: translation of the 1913 Michaelis-Menten paper. *Biochemistry*, *50*(39), 8264-8269.
- Milne, J. C., Lambert, P. D., Schenk, S., Carney, D. P., Smith, J. J., Gagne, D. J., Jin, L., Boss, O., Perni, R. B., Vu, C. B., Bemis, J. E., Xie, R., Disch, J. S., Ng, P. Y., Nunes, J. J., Lynch, A. V., Yang, H., Galonek, H., Israelian, K., Choy, W., Iffland, A., Lavu, S., Medvedik, O., Sinclair, D. A., Olefsky, J. M., Jirousek, M. R., Elliott, P. J., & Westphal, C. H. (2007). Small molecule activators of SIRT1 as therapeutics for the treatment of type 2 diabetes. *Nature*, *450*(7170), 712-716.
- Oh, K. J., Han, H. S., Kim, M. J., & Koo, S. H. (2013). Transcriptional regulators of hepatic gluconeogenesis. *Arch Pharm Res*, *36*(2), 189-200.

- Oyenihi, A. B., Langa, S. O. P., Mukaratirwa, S., & Masola, B. (2019). Effects of *Centella asiatica* on skeletal muscle structure and key enzymes of glucose and glycogen metabolism in type 2 diabetic rats. *Biomed Pharmacother*, *112*, 108715.
- Paramonov, V. M., Mamaeva, V., Sahlgren, C., & Rivero-Muller, A. (2015). Genetically-encoded tools for cAMP probing and modulation in living systems. *Front Pharmacol*, *6*, 196.
- Petersen, M. C., Vatner, D. F., & Shulman, G. I. (2017). Regulation of hepatic glucose metabolism in health and disease. *Nat Rev Endocrinol*, *13*(10), 572-587.
- Rybicka, K. K. (1996). Glycosomes--the organelles of glycogen metabolism. *Tissue Cell*, *28*(3), 253-265.
- Schnell, S. (2014). Validity of the Michaelis-Menten equation--steady-state or reactant stationary assumption: that is the question. *FEBS J*, *281*(2), 464-472.
- Stathi, A., Mamais, M., Chrysina, E. D., & Gimisis, T. (2019). Anomeric Spiro-nucleosides of beta-d-Glucopyranosyl Uracil as Potential Inhibitors of Glycogen Phosphorylase. *Molecules*, *24*(12).
- Sullivan, M. A., Aroney, S. T., Li, S., Warren, F. J., Joo, J. S., Mak, K. S., Stapleton, D. I., Bell-Anderson, K. S., & Gilbert, R. G. (2014). Changes in glycogen structure over feeding cycle sheds new light on blood-glucose control. *Biomacromolecules*, *15*(2), 660-665.
- Sullivan, M. A., Li, S., Aroney, S. T., Deng, B., Li, C., Roura, E., Schulz, B. L., Harcourt, B. E., Forbes, J. M., & Gilbert, R. G. (2015). A rapid extraction method for glycogen from formalin-fixed liver. *Carbohydr Polym*, *118*, 9-15.
- Tan, X., Sullivan, M. A., Nada, S. S., Deng, B., Schulz, B. L., & Gilbert, R. G. (2018). Proteomic Investigation of the Binding Agent between Liver Glycogen beta Particles. *ACS Omega*, *3*(4), 3640-3645.
- Thevis, M., Thomas, A., & Schänzer, W. (2010). Insulin. *Handb Exp Pharmacol*(195), 209-226.
- Wang, K., Wang, H., Liu, Y., Shui, W., Wang, J., Cao, P., Wang, H., You, R., & Zhang, Y. (2018). *Dendrobium officinale* polysaccharide attenuates type 2 diabetes mellitus via the

- regulation of PI3K/Akt-mediated glycogen synthesis and glucose metabolism. *Journal of Functional Foods*, 40, 261-271.
- Wang, Q., & Brubaker, P. L. (2002). Glucagon-like peptide-1 treatment delays the onset of diabetes in 8 week-old db/db mice. *Diabetologia*, 45(9), 1263-1273.
- Wei, S., Zhang, M., Yu, Y., Lan, X., Yao, F., Yan, X., Chen, L., & Hatch, G. M. (2016). Berberine Attenuates Development of the Hepatic Gluconeogenesis and Lipid Metabolism Disorder in Type 2 Diabetic Mice and in Palmitate-Incubated HepG2 Cells through Suppression of the HNF-4alpha miR122 Pathway. *PLoS One*, 11(3), e0152097.
- Wojtaszewski, J. F. P., Nielsen, J. N., Jørgensen, S. B., Frøsig, C., Birk, J. B., & Richter, E. A. J. B. S. T. Transgenic models – a scientific tool to understand exercise-induced metabolism: the regulatory role of AMPK (5'-AMP-activated protein kinase) in glucose transport and glycogen synthase activity in skeletal muscle. *31(6)*, 1290-1294.
- Wua, J., Wang, H. M., Li, J., & Men, X. L. (2013). [The research applications of db/db mouse]. *Sheng Li Ke Xue Jin Zhan*, 44(1), 12-18.
- Yang, H., & Yang, L. (2016). Targeting cAMP/PKA pathway for glycemic control and type 2 diabetes therapy. *J Mol Endocrinol*, 57(2), R93-R108.
- Zhang, B., Pan, Y., Xu, L., Tang, D., Dorfman, R. G., Zhou, Q., Yin, Y., Li, Y., Zhou, L., Zhao, S., Zou, X., Wang, L., & Zhang, M. (2018). Berberine promotes glucose uptake and inhibits gluconeogenesis by inhibiting deacetylase SIRT3. *Endocrine*, 62(3), 576-587.
- Zhang, Y., Chen, J., Zeng, Y., Huang, D., & Xu, Q. (2019). Involvement of AMPK activation in the inhibition of hepatic gluconeogenesis by *Ficus carica* leaf extract in diabetic mice and HepG2 cells. *Biomed Pharmacother*, 109, 188-194.
- Zhou, T., Xu, X., Du, M., Zhao, T., & Wang, J. (2018). A preclinical overview of metformin for the treatment of type 2 diabetes. *Biomed Pharmacother*, 106, 1227-1235.